[CANCER RESEARCH 64, 108–116, January 1, 2004]

Emodin Enhances Arsenic Trioxide-Induced Apoptosis via Generation of Reactive Oxygen Species and Inhibition of Survival Signaling

Jing Yi,[1] Jie Yang,[1] Rong He,[2] Fei Gao,[1] Hairong Sang,[2] Xueming Tang,[1] and Richard D. Ye[2]

[1]Department of Cell Biology, Shanghai Second Medical University, Shanghai, People's Republic of China, and [2]Department of Pharmacology, University of Illinois at Chicago, Chicago, Illinois

ABSTRACT

Although arsenic trioxide (As_2O_3) induces apoptosis in a relatively wide spectrum of tumors, the sensitivity of different cell types to this treatment varies to a great extent. Because reactive oxygen species (ROS) are critically involved in As_2O_3-induced apoptosis, we attempted to explore the possibility that elevating the cellular ROS level might be an approach to facilitate As_2O_3-induced apoptosis. Emodin, a natural anthraquinone derivative, was selected because its semiquinone structure is likely to increase the generation of intracellular ROS. Its independent and synergistic effects with As_2O_3 in cytotoxicity were studied, and the plausible signaling mechanism was investigated in HeLa cells. Cell Proliferation Assay and flow cytometry were used to assess cell viability and apoptosis. Electrophoretic mobility shift assay, luciferase reporter assay, and Western blotting were performed to analyze signaling alteration. The results demonstrated that coadministration of emodin, at low doses of 0.5–10 μM, with As_2O_3 enhanced As_2O_3-rendered cytotoxicity on tumor cells, whereas these treatments caused no detectable proproliferative or proapoptotic effects on nontumor cells. ROS generation was increased, and activation of nuclear factor κB and activator protein 1 was suppressed by coadministration. All enhancements by emodin could be abolished by the antioxidant *N*-acetyl-L-cysteine. Therefore, we concluded that emodin sensitized HeLa cells to As_2O_3 via generation of ROS and ROS-mediated inhibition on two major prosurvival transcription factors, nuclear factor κB and activator protein 1. This result allows us to propose a novel strategy in chemotherapy that uses mild ROS generators to facilitate apoptosis-inducing drugs whose efficacy depends on ROS.

INTRODUCTION

Arsenic trioxide (As_2O_3), as a therapeutic agent for acute promyelocytic leukemia and a variety of other human tumors, has been a topic of increasing interest (1–3). Although As_2O_3 induces apoptosis in a relatively wide spectrum of tumors, the sensitivity of different cell types to this treatment varies to a great extent (4, 5). For instance, among human myeloid leukemic cell lines, NB4 cells are highly sensitive, whereas HL60 and U937 cells are relatively resistant to the same dose of As_2O_3. Most of the less sensitive cancer cell lines can still be rendered apoptotic by higher doses of As_2O_3; however, these concentrations are not practical in the clinical setting (6, 7). Sensitization of the less sensitive or even resistant tumor cells to As_2O_3 may expand the therapeutic spectrum of this agent and reduce toxic side effects. This represents a challenge to investigators working on the mechanisms underlying As_2O_3-induced apoptosis.

An increasing number of studies show that cellular reductive-oxidative (redox) state might be critically relevant in the mechanism that influences cellular sensitivity to As_2O_3. For instance, cells exhibiting a low content of reduced glutathione (GSH) or low activities of glutathione *S*-transferase π, glutathione peroxidase, superoxide dismutase, and catalase are more sensitive to As_2O_3 (2, 5, 8, 9). Agents that function as either antioxidants or inhibitors and scavengers of reactive oxygen species (ROS), such as DTT and *N*-acetyl-L-cysteine (NAC), can inhibit As_2O_3-induced apoptosis (2, 5, 8, 9), whereas buthionine sulfoximine, which depletes cellular GSH, can enhance the effect of As_2O_3 (2, 5, 8, 9). Nevertheless, it has not been consistently shown that there is a direct correlation between the cellular content or activity of individual antioxidants and sensitivity to As_2O_3-induced apoptosis (5, 8, 9).

We recently found that, in several leukemic and digestive tumor cell lines, there exists an inherent difference in total amount of ROS. The inherent ROS level was positively correlated with cellular apoptotic sensitivity to As_2O_3. Moreover, through intervention with 2,3-dimethoxy-1,4-naphthoquinone (DMNQ), an agent that generates ROS intracellularly, we demonstrated that an elevation of the ROS level would sensitize cells to As_2O_3-induced apoptosis (10, 11). These results have led to the hypothesis that elevation of the cellular ROS level might be an approach to facilitate As_2O_3-induced apoptosis. In an attempt to explore this possibility, we carried out the present study. Emodin, a natural anthraquinone derivative, was selected because the derived semiquinone structure is likely to increase the generation of intracellular ROS. Its independent and synergistic effects with As_2O_3 were studied on HeLa, a human cervical epithelioid cell line. A comparison was made with the human leukemia cell line U937 and nontumor human fibroblast cells. The possible signaling mechanism was investigated. The results demonstrated that emodin, at doses causing no detectable proproliferative or proapoptotic effects on nontumor cells, sensitized tumor cells to As_2O_3 via generation of ROS and ROS-mediated inhibition of two transcription factors, nuclear factor κB (NF-κB) and activator protein 1 (AP-1).

MATERIALS AND METHODS

Cell Culture and Compounds. HeLa and U937 cells were obtained from American Type Culture Collection (Manassas, VA). Primary human skin fibroblast cells were isolated from surgically resected disposed tissue using institutionally approved protocols. HeLa and fibroblast cells were maintained in DMEM (GibcoBRL, Gaithersburg, MD), and U937 cells were maintained in RPMI 1640 (GibcoBRL), all supplemented with antibiotics and 10% fetal bovine serum. Cells were grown in a humidified atmosphere with 5% CO_2 at 37°C.

As_2O_3, emodin (6-methyl-1,3,8-trihydroxyanthraquinone), phorbol 12-myristate 13-acetate (PMA), and NAC were purchased from Sigma (St. Louis, MO). Emodin was prepared by first dissolving it in DMSO to 100 mM and then diluting it with HBSS to 1 mM. SB203580 was obtained from Calbiochem (La Jolla, CA).

Cell Viability Assay. Cells were seeded in 96-well plates at 1×10^4 cells/ml and exposed to As_2O_3, emodin, or the two-drug combination for 2–3 days, with daily change of drug-containing medium. Cell viability was assayed using CellTiter 96 AQueous Non-Radioactive Cell Proliferation Assay (MTS) Kit (Promega, Madison, WI), following the manufacturer's instructions. Absorbance at 490 nm was directly proportional to the number of living cells in culture.

Apoptosis Analysis. Apoptotic rates were analyzed by flow cytometry using Annexin V-fluorescein isothiocyarate (FITC)/propidium iodide (PI) kit (BD PharMingen, San Diego, CA), in which Annexin V bound to the apoptotic cells with exposed phosphatidylserine. Staining was performed according to the manufacturer's instructions, and flow cytometry was conducted on an

Received 10/7/02; revised 9/10/03; accepted 11/4/03.

Grant support: National Nature Science Foundation of China Grant 30170475.

The costs of publication of this article were defrayed in part by the payment of page charges. This article must therefore be hereby marked *advertisement* in accordance with 18 U.S.C. Section 1734 solely to indicate this fact.

Requests for reprints: Jing Yi, Department of Cell Biology, Shanghai Second Medical University, 280 Chongqing Road, Shanghai 200025, People's Republic of China. E-mail: yijing@shsmu.edu.cn.

Epics Elite ESP (Coulter) flow cytometer. Statistical analysis was performed using WinMDI software v. 2.8.

ROS Detection. 2,7-Dichlorodihydrofluorescein diacetate (DCFH-DA, Sigma) was used for ROS capture (5). DCFH-DA is cleaved intracellularly by nonspecific esterases and turns to highly fluorescent 2,7-dichlorofluorescein (DCF) upon oxidation by ROS. DCFH-DA working solution was added directly to the medium to reach 10 μM and then incubated at 37°C for 15 min. Cells were then washed with PBS once and kept on ice for immediate DCF detection by flow cytometer.

GSH/Oxidized Glutathione (GSSG) Ratio Assay. GSH, a tripeptide with a free thiol group, is a major antioxidant in cells. The GSH/GSSG ratio reflects the cellular redox state. Cells were trypsinized 1 h after drug treatment and prepared according to the instructions of the GSH/GSSG Ratio Assay Kit (Calbiochem). Briefly, for GSSG sample, the thiol-scavenging reagent 1-methy-2-vinylpyridinium trifluoromethanesulfonate was immediately mixed with cell suspension to eliminate GSH. Cells were frozen and thawed and then extracted with metaphosphoric acid. The cell lysates were added to GSSG or GSH assay buffers, respectively. Samples were mixed sequentially with the chromogen 5,5′-dithiobis-2-nitrobenzoic acid, glutathione reductase, and NADPH. Absorbance at 412 nm was recorded for 3 min, and the reaction rate was determined. A standard curve was constructed using a known quantity of GSH. GSH and GSSG concentrations were calculated by linear regression against the standard curve using SAS software. GSH/GSSG ratio was obtained [ratio = (GSH – 2GSSG)/GSSG].

Mitochondrial Membrane Potential ($\Delta\Psi$m) Detection. Loss of mitochondrial membrane potential was assessed by flow cytometry, using tetramethylrhodamine, ethyl ester, perchlorate (TMRE; Molecular Probes, Eugene, OR). The uptake and accumulation of TMRE in mitochondria are driven by $\Delta\Psi$m; therefore, depolarization of $\Delta\Psi$m can be represented by the loss of TMRE staining (12). The staining method was similar to that used for 2,7-dichlorodihydrofluorescein diacetate, but the final concentration for TMRE was 100 nM.

Western Blotting. After overnight starvation in serum-free medium, cells were exposed to a variety of agents. Cells were then lysed in a sample buffer containing 625 mM Tris (pH 6.8), 10% SDS, 25% glycerol, 5% β-mercaptoethanol, and 0.015% bromphenol blue, followed by sonication and heat denaturation. Proteins were loaded onto 10% SDS-PAGE gel, transferred to nitrocellulose membrane, and then detected by the proper primary and secondary antibodies before visualization by enhanced chemiluminescence (Pierce, Rockford, IL). Polyclonal antibodies against phosphorylated p38 (pTpY180/182), phosphorylated c-Jun NH_2-terminal kinase (JNK) 1 and 2/stress-activated protein kinase (pTpY183/185), and JNK1 were purchased from BioSource (Camarillo, CA), and antibody against p38 was obtained from Santa Cruz Biotechnology (Santa Cruz, CA). Antibody against IκB-α was obtained from Cell Signaling (Beverly, MA).

Luciferase Assay. Cells were transiently transfected with plasmid expression vectors containing sequences for 5× NF-κB-directed luciferase reporter or 3× AP-1-directed luciferase reporter (13, 14) using LipofectAMINE Plus reagent (Invitrogen, Carlsbad, CA) according to the manufacturer's instruction. After about 48 h, cells were exposed to a variety of agents, following overnight starvation in serum-free medium. The expression of luciferase was measured in Femtomaster FB12 luminometer (Zylux, Maryville, TN), and relative luciferase activity was acquired by normalization of transfection variation with the activity of β-galactosidase for which DNA was cotransfected. The fold increase of relative luciferase activity thereby represented the relative extent of NF-κB or AP-1 activation.

Electrophoretic Mobility Shift Assay (EMSA). After cells were starved and exposed to agents, nuclear protein extracts were prepared using a method described previously (15). Briefly, 1×10^6 cells were homogenized in NEBA buffer [10 mM HEPES (pH 7.8), 10 mM KCl, 0.1 mM EDTA, 0.1 mM EGTA, and 1 mM DTT] containing 2 μM diisopropylfluorophosphate, protease inhibitors (1× Protease Inhibitor Mixture Set I from Calbiochem), and 1 mM phenylmethylsulfonyl fluoride. Total cytosolic proteins were lysed in NEBA buffer supplemented with 0.6% NP40 and removed after centrifugation at 11,000 × g for 10 s. After homogenization of nuclei in NEBB buffer [20 mM HEPES (pH 7.8), 0.4M NaCl, 1 mM EDTA, and 1 mM EGTA], solubilized nuclear extracts were obtained after removing nuclear debris by centrifugation at 11,000 × g for 30 s. NF-κB and AP-1 oligonucleotide probes (Promega) were labeled with ^{32}P according to the manufacturer's instruction. Nuclear extract samples bound with labeled probes were loaded onto a 6% acrylamide gel. After electrophoresis, the gel was dried, and autoradiograph was exposed using a PhosphorImager cassette for 4 days at room temperature and then scanned and analyzed using ImageQuant software version 3.3 (Molecular Dynamics) as described previously (15).

IκB-α Dominant Negative Mutant Transfection. Overexpression of an IκB-α dominant negative mutant (32/36 serine) unable to be phosphorylated like a wild-type IκB-α will block the activation of NF-κB. Cells were transiently transfected with plasmid expression vectors containing an IκB-α dominant negative mutant [IκB-DM (14, 15)] using the above-mentioned LipofectAMINE method. Nonrelevant plasmid pcDNA3 was used as transfection control. Forty-eight h after transfection, cells were exposed to drugs for another 3 days. Annexin V-phycoerythrin/PI double staining flow cytometry was performed to determine apoptosis and to investigate the role of NF-κB in apoptosis.

Statistics. SAS6.12 software was used for statistical analysis. Student's t test was applied for comparison of the means of two groups, and ANOVA was used for the means of multiple groups. For all of the value differences, $P < 0.05$ was considered significant.

RESULTS

Inhibition of Cell Viability in Tumor Cells but not in Nontumor Cells. In HeLa cells, low doses of emodin, ranging from 2 to 10 μM, caused a slight reduction in the number of viable cells in culture (Fig. 1*A*). Cell number reduction in HeLa cells was attributed mainly to a mild inhibition of cell proliferation because the apoptosis assay did not display discernable cell death when treated with <10 μM emodin (Fig. 2*B*). Cotreatment with 10 μM emodin apparently sensitized U937 cells to As_2O_3-induced cytotoxicity. Similar treatment had no effect on fibroblast cells (Fig. 3).

Enhancement of As_2O_3-Induced Apoptosis. Emodin, at low doses ranging from 0.5 to 10 μM, facilitated As_2O_3 cytotoxicity in a dose-dependent fashion in HeLa cells (Fig. 1*B*, Fig. 2, and Fig. 3). Of

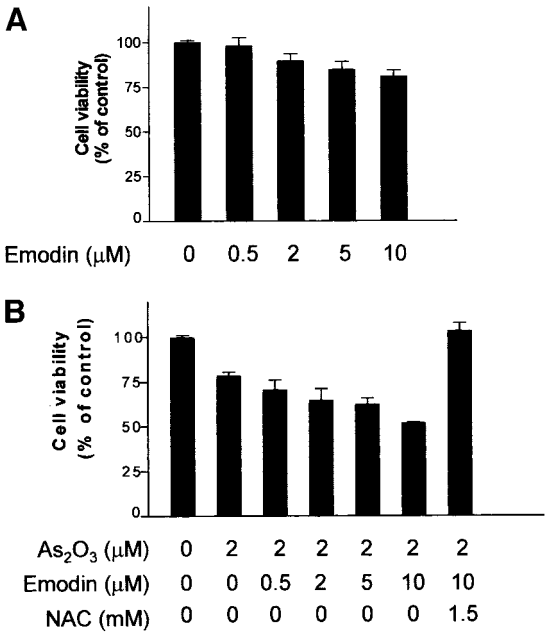

Fig. 1. Cell viability assays (MTS) in HeLa cells treated with emodin (*A*) and As_2O_3 with or without emodin or plus *N*-acetyl-L-cysteine (*B*). Drug-containing medium in 96-well plates was changed daily for 3 days before MTS was performed. Twenty μl of reactive mixture were added to each well and incubated with cells at 37°C for 2 h. Cell viability was modestly decreased in emodin-treated samples in a dose-dependent way (*A*). As_2O_3 caused an inhibition in cell viability, whereas emodin potentiated As_2O_3-induced viability decrease in a dose-related fashion, and the antioxidant *N*-acetyl-L-cysteine completely prevented this decrease (*B*). Each sample was triplicated, and experiments were repeated three times.

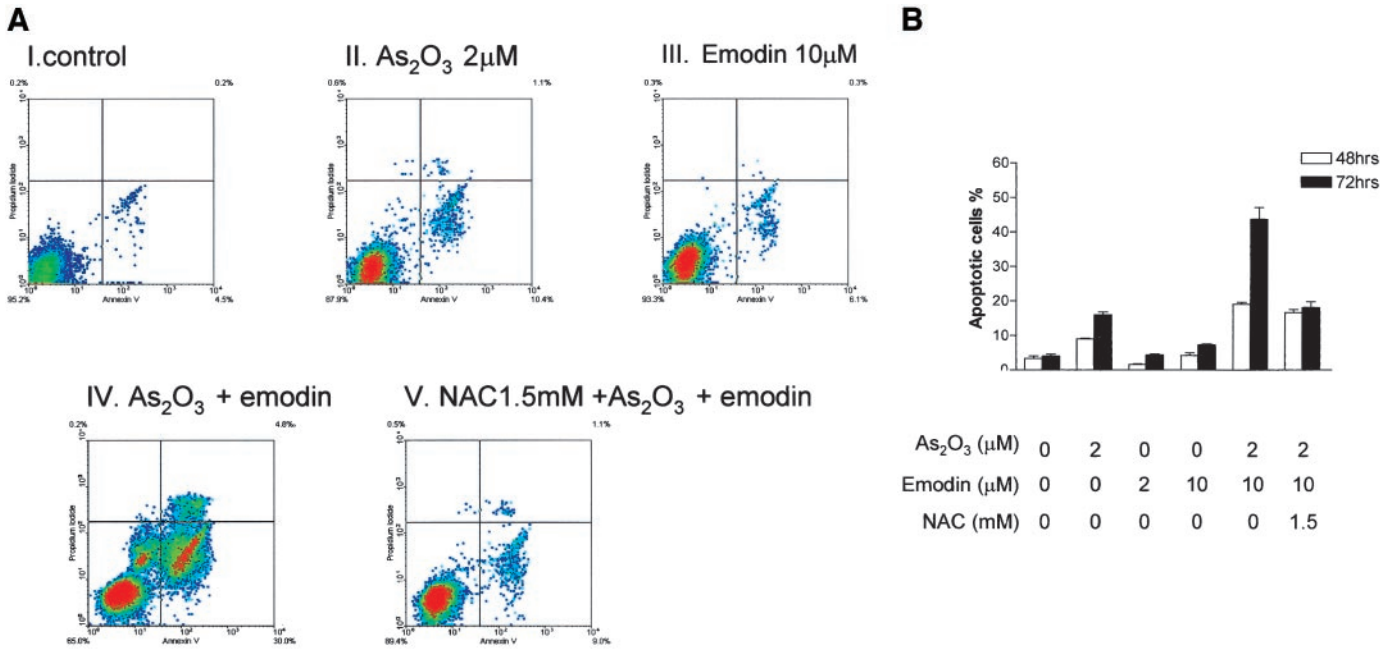

Fig. 2. Apoptosis rate analysis using Annexin V/propidium iodide flow cytometry in HeLa cells treated with As_2O_3, emodin, the two-drug combination, or the two-drug combination + *N*-acetyl-L-cysteine. Density plots, *A*; bar chart, *B*. Drug-containing medium was changed daily for 2 or 3 days. Cells were trypsinized before incubation with Annexin V and propidium iodide for 15 min at room temperature. Apoptotic cells, represented by Annexin V-positive cells, increased significantly in two-drug combination-treated samples on the third day, compared with samples treated with As_2O_3 only. *N*-Acetyl-L-cysteine rescued two-drug combination-induced apoptosis. Each sample was duplicated, and the data represent the results of four assays.

interest, emodin at 0.5 μM caused no appreciable change in either cell proliferation or death (Fig. 1*A*). However, when this dose was coadministered with 2 μM As_2O_3, it enhanced As_2O_3-induced cytotoxicity (Fig. 1*B*). This cytotoxicity consists of an inhibition of cell proliferation and an induction of apoptosis, the latter of which is depicted by Annexin V/PI flow cytometry (Fig. 2).

Decrease of Mitochondrial Membrane Potential. The two-drug combination caused more HeLa cells to undergo a reduction in mitochondrial membrane potential ($\Delta\Psi$m) because the cell population with relatively low TMRE staining became predominant in the samples exposed to both drugs (Fig. 4). This indicates that the effect of emodin in enhancing As_2O_3-induced apoptosis in HeLa cells involves a decrease of mitochondrial membrane potential, which is the identical event that occurs in As_2O_3-induced apoptosis (2).

Dependence on ROS Level and Redox State. Exposure of HeLa cells to emodin elicited an immediate elevation of cellular ROS level.

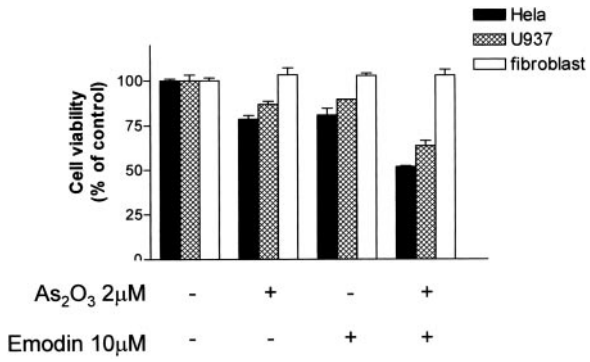

Fig. 3. Cell viability assay (MTS) in HeLa, U937, and fibroblast cells treated with As_2O_3, emodin, or the two-drug combination. As_2O_3 and emodin, used for 3 days, resulted in a decrease in cell viability in HeLa and U937 cells, and the two-drug combination significantly potentiated As_2O_3-induced viability reduction in these two cell lines. However, cell viability was not affected in fibroblast cells. Each sample was triplicated, and experiments were repeated twice.

This elevation occurred more rapidly and to a greater extent than that caused by As_2O_3 but rapidly returned to normal. Cotreatment with emodin and As_2O_3 dramatically augmented ROS level elevation (Fig. 5).

Because emodin has been reported to have fluorescent properties (16), we excluded its background fluorescence when determining ROS by the measurement of DCF fluorescence. Results showed that at the doses used in this study, its fluorescence was below the detectable level (data not shown).

The GSH/GSSG ratio showed that the combination of emodin and As_2O_3 had a remarkable oxidative impact on cellular redox state. Its effect on reduction of the GSH/GSSG ratio involved both an increase of GSSG and a decrease of GSH (Fig. 6).

NAC, an aminothiol and synthetic precursor of intracellular cysteine and GSH, is known as a general antioxidant. Its modes of action include scavenging ROS and increasing the intracellular level of GSH (17, 18). Pre- or cotreatment of cells with 1.5 mM NAC for 24 h partially abolished the elevation of ROS and the decrease of the GSH/GSSG ratio caused by the two-drug combination (Figs. 5 and 6). Cotreatment with NAC also attenuated apoptosis and the collapse of $\Delta\Psi$m caused by emodin in combination with As_2O_3 (Figs. 1, 2, and 4). These data indicated that emodin's enhancement of As_2O_3-inducing cytotoxicity was dependent on ROS.

Inhibition of NF-κB and AP-1 Activation. To explore whether the activation of transcription factors was altered in emodin/As_2O_3-induced apoptosis, the activation of NF-κB and AP-1 was evaluated using EMSA and transcription factor-driven luciferase reporter assay. The simple administration of As_2O_3 or emodin failed to visualize a discernable change in NF-κB activation, as displayed by EMSA and luciferase assay (Fig. 7). Luciferase assay for AP-1 activation did not show change either (data not shown). These data excluded the fact that these treatments evoked any significant activation on NF-κB or AP-1. We then proposed to determine whether the drugs had an inhibitory effect on transcription factor activation. To accomplish this experi-

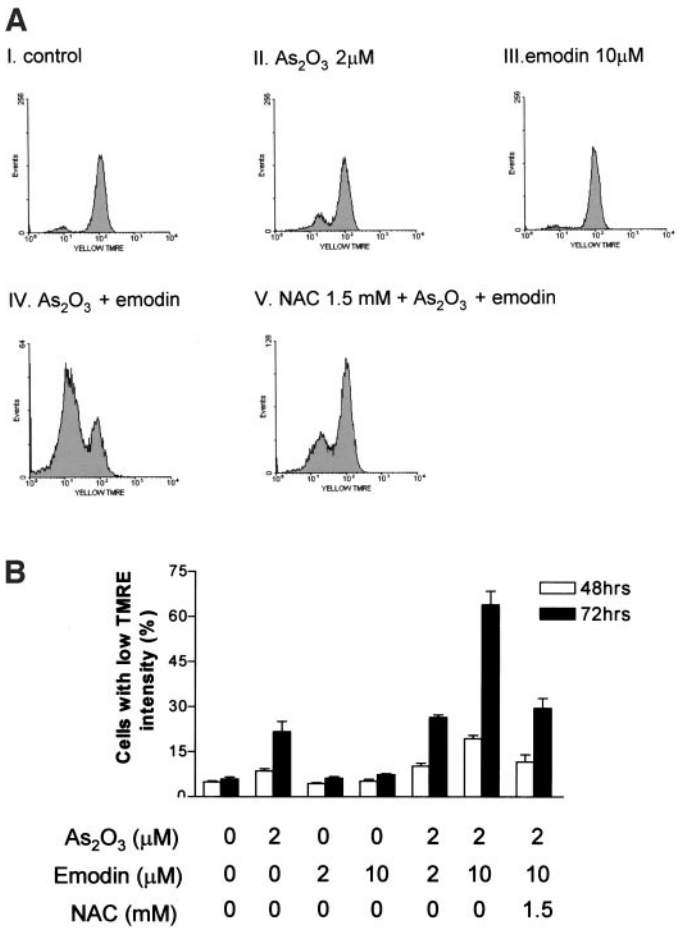

Fig. 4. Tetramethylrhodamine, ethyl ester, perchlorate (TMRE) flow cytometry assessing the collapse of mitochondrial membrane potential ($\Delta\Psi$m) in HeLa cells treated with As_2O_3, emodin, the two-drug combination, or the two-drug combination + *N*-acetyl-L-cysteine. Histograms, *A*; bar chart, *B*. Cells were treated with drugs before staining with TMRE. Cells that were losing or had lost $\Delta\Psi$m were less stained or unstained. The two-drug combination resulted in a dramatic increase of the cell population with low TMRE intensity, and this was prevented by *N*-acetyl-L-cysteine. Each sample was duplicated, and experiments were repeated three times.

ment, it was necessary to use an agent that stimulates the activation of NF-κB and AP-1 because it was not possible to observe inhibition of the low basal levels without stimulation (see Fig. 7). Therefore, cells were pretreated with As_2O_3 and/or emodin, followed by PMA stimulation. PMA was chosen because, as a phorbol ester and typical mitogen, it generally stimulates NF-κB and AP-1 activation without triggering the direct apoptotic events. Also, the doses and timing of PMA treatment applied in this study proved not to change ROS level (data not shown).

EMSA (Fig. 8*A*) showed that PMA-stimulated NF-κB activation was slightly suppressed by As_2O_3, and this suppression was enhanced by cotreatment with emodin, although emodin itself did not cause suppression of NF-κB activation during this short treatment (45 min). Luciferase assay (Fig. 8*C*) showed that emodin itself also inhibited PMA-stimulated NF-κB activation when it worked on cells for longer time (4 h), whereas cotreatment with emodin and As_2O_3 further potentiated the suppression of PMA-stimulated NF-κB activation. In addition, we showed that the cytoplasmic quantity of IκB-α was increased on two-drug coadministration, which indicated that inhibition of NF-κB activation caused by As_2O_3 + emodin might involve the inhibition of IκB-α degradation (Fig. 8*B*). Again, inhibition of NF-κB activation by emodin + As_2O_3 could be partially abolished by the antioxidant NAC (Fig. 8).

As demonstrated by EMSA, PMA-elicited AP-1 activation was remarkably suppressed by cotreatment with As_2O_3 + emodin, despite the fact that neither As_2O_3 nor emodin alone inhibited AP-1 activation at that moment [45 min (Fig. 9*A*)]. Luciferase assay indicated that, by 4 h of treatment, emodin caused a slight inhibition of PMA-stimulated AP-1 activation, and two-drug combination showed a stronger inhibition (Fig. 9*B*). Similar to the case of NF-κB, the inhibition on AP-1 activation by emodin + As_2O_3 could be abolished by the antioxidant NAC (Fig. 9).

Prosurvival Role of NF-κB. To determine the role of NF-κB activation in emodin/As_2O_3-induced apoptosis, we first studied the effect of PMA on these drugs. Cell viability assay showed that cotreatment of PMA with the drugs increased cellular resistance to the cytotoxic effect of these drugs (Fig. 10*A*). This indirectly indicated a prosurvival role of NF-κB activation because PMA stimulated NF-κB activation. We further verified this role by transient transfection of a dominant negative IκB-α mutant to block the activation of NF-κB. Annexin V/PI flow cytometry showed that cells transiently transfected with dominant negative IκB-α mutant were more sensitive to apoptosis induced by As_2O_3 and the emodin + As_2O_3 combination (Fig. 10*B*). These results suggested that NF-κB activation plays a prosurvival or antiapoptotic role.

Activation of Stress Response Kinases. To determine the signal transduction pathway between ROS elevation and transcription factor inhibition, we investigated the activation patterns of p38 kinase, JNK, and extracellular signal-regulated kinase 1/2, all three of which are known to be activated in response to oxidative stress. Results showed that p38 was mildly activated by As_2O_3, but not by emodin, whereas coadministration of the two drugs resulted in a potentiated activation. Antioxidant NAC could attenuate this potentiated activation (Fig. 11*A*). Therefore, p38 activation was involved in As_2O_3-induced and emodin-enhanced apoptosis. Surprisingly, JNK activation was not affected by either treatment (Fig. 11*B*). The extracellular signal-regulated kinase 1/2 activation was not influenced by drug treatment either (data not shown).

To investigate preliminarily whether p38 activation is required for the cytotoxicity of the two-drug combination, we use SB203580, a

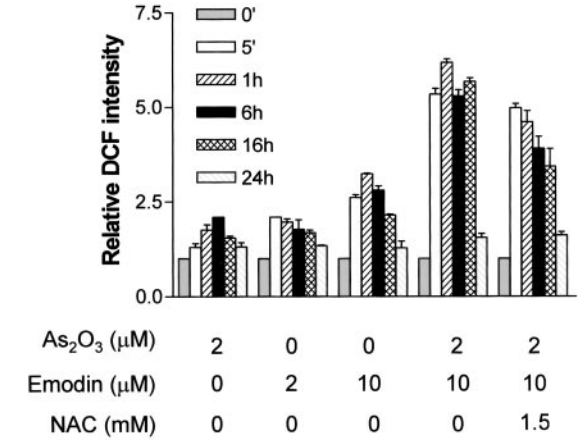

Fig. 5. Time course for reactive oxygen species (ROS) level detected by 2,7-dichlorodihydrofluorescein flow cytometry in HeLa cells with a variety of treatments. HeLa cells were exposed to As_2O_3, emodin, the two-drug combination, or the two-drug combination + *N*-acetyl-L-cysteine (NAC) for the indicated times and doses. NAC, where applied, was incubated with cells for 24 h. For ROS capture, 2,7-dichlorodihydrofluorescein diacetate was incubated with cells at 37°C for 15 min before cells were harvested. Cellular ROS level, as reflected by relative DCF intensity, had a more rapid and slightly higher elevation in emodin-treated samples than in As_2O_3-treated ones. The two-drug combination significantly augmented ROS elevation. NAC attenuated the two-drug-potentiated ROS elevation. Each sample was duplicated, and the figure is representative of four assays.

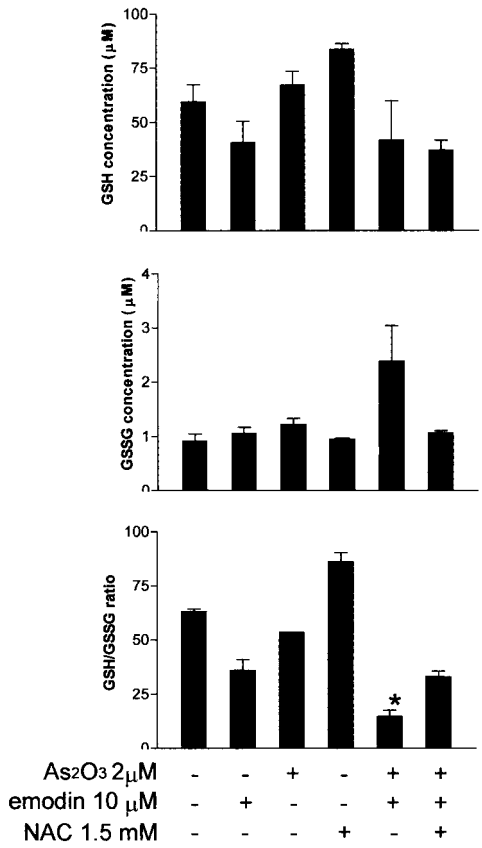

Fig. 6. Reduced glutathione (GSH)/oxidized glutathione (GSSG) ratio assay. HeLa cells were exposed to As_2O_3, emodin, the two-drug combination, or the two-drug combination + *N*-acetyl-L-cysteine (NAC) for 1 h. NAC was incubated with cells for 24 h before drug treatment. Emodin caused a moderate decrease of the GSH/GSSG ratio. The two-drug combination raised the GSSG concentration and caused a dramatic decrease in the GSH/GSSG ratio. * indicates that the value differences of the two-drug combination *versus* As_2O_3 alone or *versus* the two-drug combination + NAC were significant ($P = 0.0025$). Each sample was quadruplicated, and the figure is representative of two assays.

specific and cell-permeable inhibitor of p38 kinase, as the cotreatment with the drugs before the assessment of cell viability. Twenty μM was chosen as an effective inhibitory dose for p38 activation, based on a Western blot assessment (data not shown). Results showed that the inhibition of p38 activation did not protect cells from cytotoxicity (Fig. 11*C*).

DISCUSSION

Based on our previous studies that the inherent cellular level of ROS may be positively related to the susceptibility of the tumor cells to As_2O_3 and that a naphthroquinone, DMNQ, sensitizes cells to As_2O_3-induced apoptosis (10, 11), we tried to search for a natural anthraquinone that may exert an effect similar to that of DMNQ. We proved in the present study that emodin, at doses causing no detectable proproliferative or proapoptotic effects on nontumor cells, sensitized tumor cells to As_2O_3-induced apoptosis through elevation of intracellular ROS level and inhibition of the survival mechanisms, *i.e.*, activation of NF-κB and AP-1.

It has been known that emodin had some effects on inhibition of cell proliferation or induction of cell death (19–21), thus it may function in suppression of tumor growth or inflammation (22, 23), although the underlying mechanisms are not well elucidated. Two recent findings on emodin's antitumor effect are that it can selectively work on neuroectodermal tumors (16) and preferentially suppress the transformation of HER2/neu-overexpressing breast cancer cells by inhibiting HER2/neu tyrosine kinase activity (24).

We noticed that in the literature, emodin, when used alone, requires a high dose (approximately 40 μM or higher) to achieve its inhibitory effect on cell proliferation or induction of cell death. Our preliminary test showed that emodin alone exerted a significant proapoptotic effect on HeLa cells at a dose starting from 30 μM, and these doses showed cytotoxicity to normal fibroblast cells (data not shown). We thereby selected a dose range that caused no appreciable effect on nontumor cells. Emodin alone at these doses (*i.e.*, 0.5–10 μM) induced mild inhibition of tumor cell proliferation in a dose-dependent fashion, whereas the effect on cell death was negligible at concentrations below 10 μM. However, when emodin at these doses (typically at 10 μM) was coadministered with 2 μM As_2O_3, it enhanced As_2O_3-induced apoptosis in HeLa and U937 cells. Of note, the apoptosis rate achieved by the two-drug combination was similar to that achieved by 5 μM As_2O_3 (data not shown), whereas this high dose of As_2O_3 is not clinically acceptable (7). Pecere *et al.* (16), in their studies of aloe-

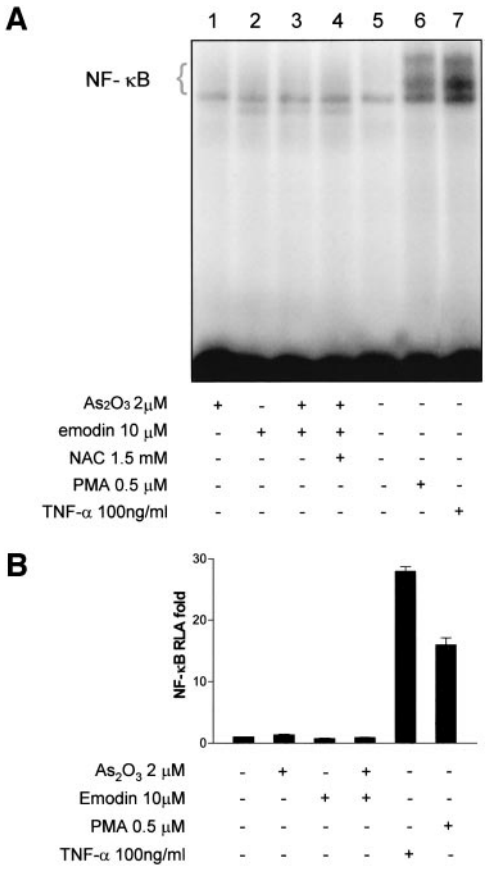

Fig. 7. Assays for nuclear factor κB (NF-κB) activation in HeLa cells treated with As_2O_3, emodin, the two-drug combination, or the two-drug combination + *N*-acetyl-L-cysteine (NAC). Electrophoretic mobility shift assay (EMSA), *A*; luciferase assay, *B*. Cells were starved overnight before treatment with the drugs and reagents for 45 min, except that NAC was incubated with cells for 16 h before drug treatment. Cells were then harvested for EMSA. Result of EMSA (*A*) showed that NF-κB activation, indicated by its translocation to nuclei and binding to the specific sites on DNA, yields multiple shifted bands on the gel of EMSA (see *Lanes 6* and *7*). As_2O_3 (*Lane 1*), emodin (*Lane 2*), the two-drug combination (*Lane 3*), or the two-drug combination + NAC (*Lane 4*) did not change the basal level of NF-κB activation (*Lane 5*). Phorbol 12-myristate 13-acetate (PMA)- and tumor necrosis factor α (TNF-α)-stimulated samples served as the positive controls (*Lanes 6* and *7*). In the luciferase assay, cell treatments were given at 48 h posttransfection. After overnight starvation, cells were treated with the drugs and reagents and then harvested after 4 h of incubation. Results (*B*) showed that As_2O_3, emodin, and the two-drug combination (*bars 2–4* from the *left*) did not affect the basal level of NF-κB-related relative luciferase activity (*bar 1*), compared with positive controls PMA and TNF-α (*bars 5* and *6*). Experiments were repeated two (EMSA) or four (luciferase assay) times.

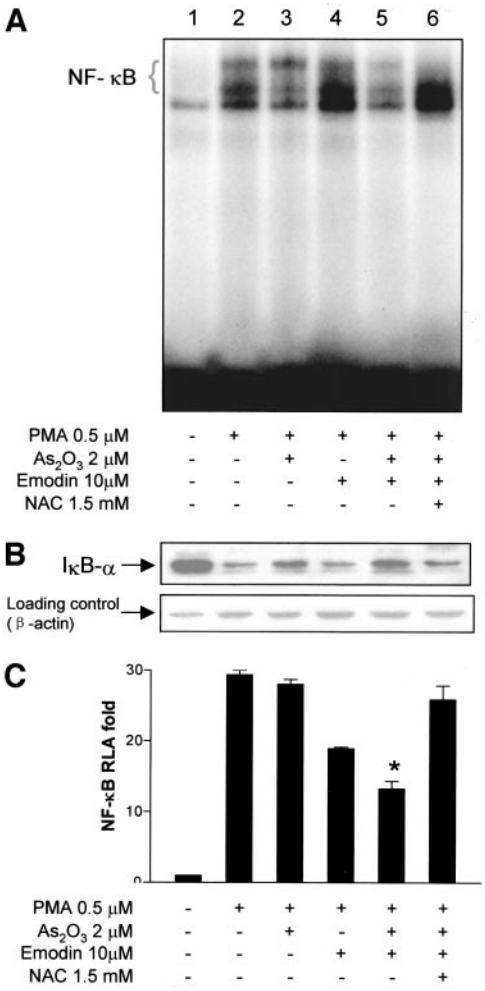

Fig. 8. Assays for nuclear factor κB (NF-κB) activation in HeLa cells pretreated with As_2O_3, emodin, the two-drug combination, or the two-drug combination + *N*-acetyl-L-cysteine (NAC) and stimulated with phorbol 12-myristate 13-acetate (PMA). Electrophoretic mobility shift assay (EMSA), *A*; Western blotting for IκB-α, *B*; luciferase assay, *C*. Cells were starved overnight. NAC, where applied, was added 16 or 24 h before other agents. In EMSA, after pretreatment with As_2O_3, emodin, the two-drug combination, or the two-drug combination + NAC for 30 min, cells were stimulated with PMA (500 nM) for 45 min. Results of EMSA (*A*) showed that NF-κB binding to DNA (*i.e.*, activation of NF-κB) was induced by PMA (*Lane 2*). Whereas this activation was slightly inhibited by As_2O_3 (*Lane 3*), but not by emodin (*Lane 4*), the two-drug cotreatment rendered a remarkable inhibition (*Lane 5*). NAC abolished the two-drug-rendered inhibition of NF-κB activation (*Lane 6*). In the luciferase assay, cell treatments were given at 48 h posttransfection. After overnight starvation and pretreatment with the drugs for 30 min, PMA was added for a 4-h incubation. Results (*C*) showed that PMA-stimulated NF-κB activation (*bar 2*) was inhibited by emodin alone (*bar 4*) and significantly further inhibited by the two-drug combination (*bar 5*). In Western blot for IκB-α, after the 30-min pretreatment, cells were stimulated with PMA for 30 min before harvest. Results (*B*) showed that the decrease of IκB-α was accompanied by PMA-induced NF-κB activation (*Lane 2*). Whereas this decrease of IκB-α was slightly inhibited by As_2O_3 (*Lane 3*), but not by emodin (*Lane 4*), the two-drug cotreatment rendered a remarkable inhibition (*Lane 5*). NAC abolished the two-drug-rendered inhibition on IκB-α decrease (*Lane 6*). Experiments were repeated two to four times. * indicated that the value differences of *bar 5 versus bar 4* or *versus bar 6* were significant ($P = 0.0006$).

emodin cytotoxicity on a variety of cell lines, considered HeLa cells to be insensitive to this drug (used at 50 μM). However, our results show that treatment of HeLa cells with a relatively lower dose of emodin (10 μM) + As_2O_3 rendered HeLa cells as sensitive to apoptosis as the neuroectodermal tumor cells and other sensitive cells classified in the study of Pecere *et al.* (16). Exposure of U937 cells to As_2O_3 + emodin made this originally "insensitive" cell line sensitive to As_2O_3 and therefore further confirmed the synergistic efficacy of emodin.

Emodin, a component of plant extracts used to make laxative products, is a type of natural anthraquinone with a molecular structure similar to that of DMNQ (20). DMNQ is considered a ROS generator because its property of quinone and derived semiquinone, like mitochondrial ubiquinone, allows it to transfer electrons (25–27). Emodin has a structure similar to those of DMNQ and ubiquinone (shown in Fig. 12), but its capability to generate ROS has not been adequately studied (28), nor has a link between its anticancer effect and ROS generation been established. We found in the present study that emodin elicited an immediate elevation of cellular ROS level and a moderate reduction of the GSH/GSSG ratio. Compared with the ROS fluctuation related to As_2O_3, emodin-triggered ROS elevation was more potent and rapid but transient. Remarkably, emodin augmented As_2O_3-induced ROS elevation when it was coadministered. As_2O_3 increases cellular ROS through an unknown mechanism that may be related to the disruption of mitochondrial respiration chain (2, 29, 30). In contrast, emodin seems to elevate ROS level by direct generation of ROS, as reflected by the pattern of emodin-related ROS fluctuation

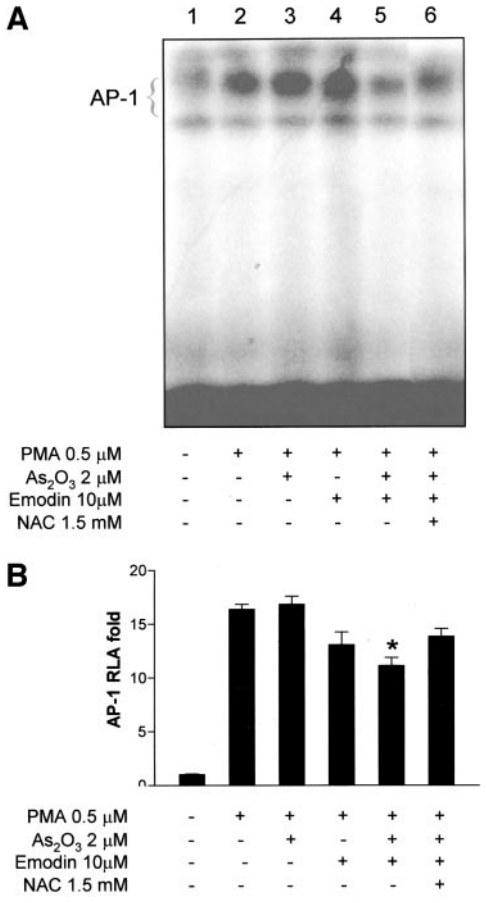

Fig. 9. Assays for activator protein 1 (AP-1) activation in HeLa cells pretreated with As_2O_3, emodin, the two-drug combination, or the two-drug combination + *N*-acetyl-L-cysteine (NAC) and stimulated with phorbol 12-myristate 13-acetate (PMA). Electrophoretic mobility shift assay (EMSA), *A*; luciferase assay, *B*. Cells were starved overnight. NAC, when applied, was added 16 or 24 h before other agents. In EMSA, after pretreatment with drugs for 30 min, cells were stimulated with 500 nM PMA for 45 min. Results of EMSA (*A*) showed that AP-1 binding to DNA (*i.e.*, activation of AP-1), reflected by a predominant band, was induced by PMA (*Lane 2*). Whereas this activation was not significantly altered by either As_2O_3 (*Lane 3*) or emodin (*Lane 4*), the two-drug cotreatment rendered a remarkable inhibition (*Lane 5*). NAC abolished the two-drug-rendered inhibition of AP-1 activation (*Lane 6*). In the luciferase assay, cell treatment was given at 48 h posttransfection. After overnight starvation and pretreatment with the drugs for 30 min, PMA was added for a 4-h incubation. Results (*B*) showed that PMA-stimulated AP-1 activation (*bar 2*) was inhibited by emodin alone (*bar 4*) and further inhibited by the two-drug combination (*bar 5*). NAC partially abolished this inhibition. Experiments were repeated two to four times. * indicated that the value differences of *bar 5 versus bar 4* or *versus bar 6* were significant, although statistically marginal ($P = 0.073$).

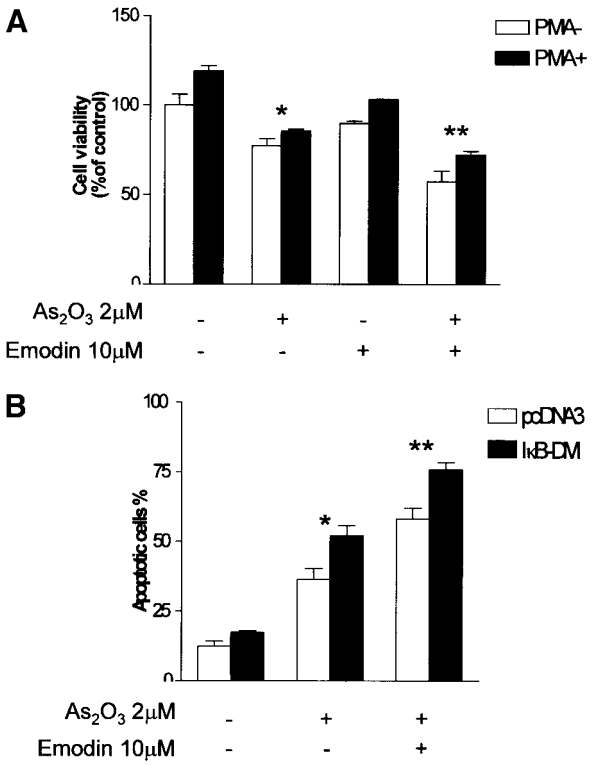

Fig. 10. Assays to determine the role of nuclear factor κB activation in cellular susceptibility to cytotoxicity of As_2O_3, emodin, and the two-drug combination. MTS, *A*; Annexin V/propidium iodide flow cytometry on dominant negative IκB-α mutant-transfected cells, *B*. Cells were exposed to As_2O_3, emodin, and the two-drug combination with or without 500 nM phorbol 12-myristate 13-acetate (PMA) for 3 days before MTS assay. Cell viability rate was higher in PMA-treated cells. * and ** indicated that values of PMA+ *versus* PMA− were significantly different ($P = 0.004$ and 0.014; *A*). For apoptosis assay, dominant negative IκB-α mutant (*IκB-DM*) was transfected 40 h before drug treatment for 3 days. Annexin V/propidium iodide flow cytometry showed the increased apoptotic rate in IκB-DM-transfected cells on drug exposure, compared with the control DNA-transfected cells. * and ** indicated that values of IκB-DM+ *versus* IκB-DM− were significantly different ($P = 0.007$ and 0.020; *B*). Each sample was quadruplicated (MTS) or duplicated (flow cytometry), and assays were repeated twice.

and redox state. Emodin's enhancement of As_2O_3-induced cytotoxicity in HeLa cells is apparently dependent on ROS generation because the enhancement of both proliferation-inhibition and apoptosis rendered by cotreatment with the two drugs can be abolished or attenuated by the antioxidant NAC.

ROS-dependant regulation of signaling and transcription activation has become a focus of a large body of investigation (31–33). It is known that AP-1, one of the first mammalian transcription factors to be identified, and NF-κB, another important transcription factor, can be regulated by a variety of physiological and pathological stimuli, including changes in cellular redox state. These transcription factors, in turn, regulate a wide range of cellular activities, including cell proliferation, differentiation, and death. In response to an oxidative stress, activated mitogen-activated protein kinase members translocate to the nucleus to phosphorylate and thereby potentiate the activity of the components of these so-called redox-sensitive transcription factors (7, 33–38). On the other hand, activation of these transcription factors may be inhibited by overloaded oxidants that oxidize the cysteine residues within the DNA-binding region of transcription factors (31). Activation of NF-κB and AP-1 is predominantly thought to serve as a prosurvival factor (34–38), although these transcription factors are involved in both proliferation and apoptosis events (34–40). Inhibition of their activation may hence shift the survival/death control (35, 38, 41). In the present study, PMA, a typical phorbal ester and strong mitogen, activates NF-κB and AP-1 in HeLa cells and increases cellular resistance to the cytotoxicity of the two drugs. Blockage of NF-κB activation by transfection of a dominant negative IκB-α mutant potentiates cellular susceptibility to drug cytotoxicity. This indicated that NF-κB and AP-1 activation, served as prosurvival or antiapoptotic forces, was suppressed by cotreatment with emo-

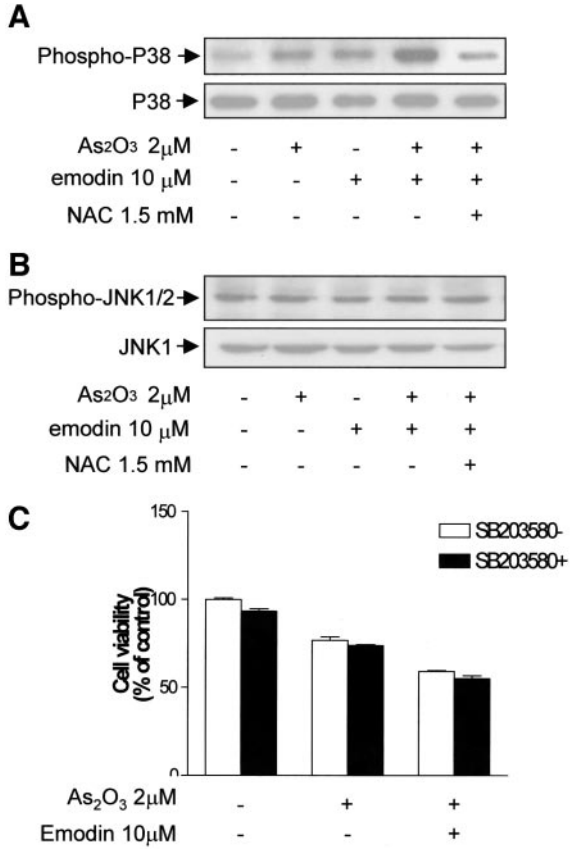

Fig. 11. Mitogen-activated protein kinase activation in HeLa cells treated with As_2O_3, emodin, the two-drug combination, or the two-drug combination + *N*-acetyl-L-cysteine. Western blots, *A* and *B*; MTS, *C*. For Western blots, cells were starved overnight and then incubated with drugs for 10 min. Results showed that p38 was mildly activated by As_2O_3, and cotreatment with emodin potentiated the activation of p38. *N*-Acetyl-L-cysteine abolished emodin's enhancement (*A*). However, c-Jun NH_2-terminal kinase activation was affected by neither As_2O_3, emodin, nor the two-drug combination (*B*). Western blot experiments were repeated three times. For cell viability assay, SB203580 (20 μM), the inhibitor of p38, was added with the drugs. MTS results (*C*) showed that inhibition of p38 activation did not protect cells from the cytotoxicity rendered by As_2O_3 or the two-drug combination. The value differences between SB203580+ and SB203580− samples in each group were statistically insignificant ($P = 0.996$). Each sample was quadruplicated.

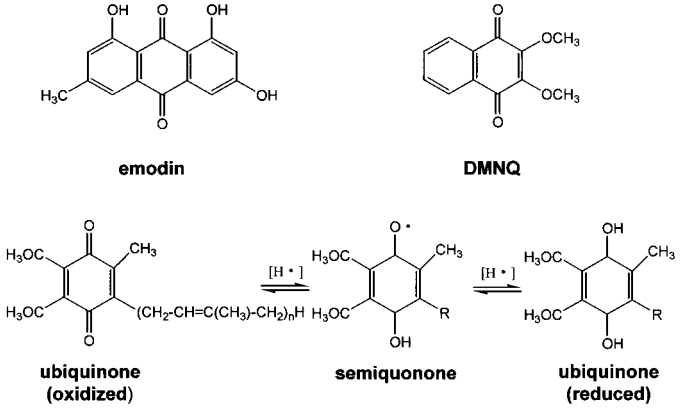

Fig. 12. Structures of emodin, 2,3-dimethoxy-1,4-naphthoquinone (*DMNQ*), and mitochondrial ubiquinone.

din + As_2O_3, whereas As_2O_3 or emodin alone had no suppressive effect or little suppressive effect. This synergistic suppression may be attributed, at least in part, to the substantial increase of cellular ROS and the dramatic oxidative stress resulting from the two-drug cotreatment because NAC prevented this effect.

Among the three types of mitogen-activated protein kinases, p38 and JNK/stress-activated protein kinase are predominantly activated in response to cellular redox stress (32, 34). In our study, p38 phosphorylation was moderately activated by As_2O_3, and this activation was enhanced by emodin. Conversely, JNK activation was not. The role of JNK in mediation of apoptosis has been emphasized in an increasing number of recent reports (34, 42–44). JNK activation and, consequently, c-Jun phosphorylation usually precede AP-1 activation. In other words, suppression of AP-1 could be linked to inactivation of JNK. In the present study, the activation of p38, but not JNK, seemed to be involved in ROS-mediated enhancement of cytotoxicity, although the activation of p38 was not necessarily required for cytotoxicity. However, NF-κB and AP-1 may regulate their activity by sensing changes in the intracellular redox state, rather than by merely recognizing redox-related upstream signals (*i.e.*, mitogen-activated protein kinases). Evidence exists implying that ROS may have opposite effects on upstream mitogen-activated protein kinase signaling systems *versus* downstream transcription factors [*i.e.*, they activate different families of protein kinases and, on the other hand, oxidize the cysteine residues within the DNA-binding region of transcription factors that result in their inactivation (31)]. In our work, emodin in combination with As_2O_3 exerted remarkable ROS-mediated suppression of two antiapoptosis transcription factors, and this appears to be responsible for the enhanced cytotoxicity rendered by cotreatment with the two drugs.

Previous studies showed that emodin inhibits tumor cell growth and sensitizes tumor cells to chemotherapy through the inhibition of tyrosine kinase activation (24). Activation of extracellular signal-regulated kinase, p38, and JNK all required tyrosine kinase for phosphorylation of their tyrosine residues. In the present study, activation of mitogen-activated proteins apparently was not inhibited by emodin alone or emodin + As_2O_3 at the doses used. Therefore, inhibition of tyrosine kinase certainly does not account for the effect of emodin in the present case.

It has been known that cellular ROS is essential to cell survival, but the effect of ROS on cells is complex. Experimentally, a low concentration of H_2O_2 causes a modest increase in proliferation of many tumor cell lines, whereas a higher level results in slowed growth, cell cycle arrest, and apoptosis or even necrosis (45). This implies that the effects of ROS are determined by their levels. This can explain the fact that arsenic, which was initially recognized as an environmental carcinogen, becomes an anticancer agent by inducing apoptosis of tumor cells (7). Our results suggest that when emodin is coadministered with As_2O_3, the elevation of ROS may surpass a certain threshold that finally overcomes antiapoptosis forces and promotes a shift of the survival/death balance to death. Interestingly, when the drugs were added to cells, ROS elevation occurred immediately and subsided by about 24 h, and the ROS-mediated kinase activation and transcription factor suppression were induced shortly, whereas apoptosis occurred late on the second or third day. This implies that the elevation of ROS level, acting as a secondary signal, quickly triggers an alteration in survival/death signaling and fulfills its impact on the final destiny of the cell. Because the extent of synergized cytotoxicity is linked to the inherent cellular ROS level, tumor cells are more subject to this effect because they usually bear a higher ROS level than their nontumor counterparts. This explains the nonresponsiveness of fibroblast cells to the two-drug coadministration.

Thus far, antioxidants have been considered helpful in cancer treatment because they reduce the side effects of chemo- and radiotherapy (46). We demonstrate in this article that emodin, a natural anthraquinone, enhances As_2O_3-induced apoptosis via generation of ROS and ROS-mediated inhibition of survival signaling. Herein we propose a novel strategy in which emodin and other ROS-generating agents may serve as the enhancer in chemotherapy, synergizing the drugs that depend on ROS. Given that ROS generation is increased predominantly in transformed cells, nontumor cells, which have a relatively lower inherent ROS level, can be unsusceptible to coadministration. Thus, this strategy may be advantageous in terms of the modest side effects, especially under the circumstances that ROS-generating agents are derived from natural plants and used with low doses. Future investigation should address the detailed pathways by which these synergizing drugs are involved in overriding the antiapoptotic forces.

ACKNOWLEDGMENTS

We thank Phoebe Lin for constructive reading of the manuscript.

REFERENCES

1. Miller, W. H., Jr., Schipper, H. M., Lee, J. S., Singer, J., and Waxman, S. Mechanisms of action of arsenic trioxide. Cancer Res., *62:* 3893–3903, 2002.
2. Chen, Z., Chen, G. Q., Shen, Z. X., Chen, S. J., and Wang, Z. Y. Treatment of acute promyelocytic leukemia with arsenic compounds: *in vitro* and *in vivo* studies. Semin Hematol., *38:* 26–36, 2001.
3. Wang, Z. Y. Arsenic compounds as anticancer agents. Cancer Chemother. Pharmacol., *48* (Suppl. 1)*:* S72–S76, 2001.
4. Akao, Y., Yamada, H., and Nakagawa, Y. Arsenic-induced apoptosis in malignant cells *in vitro*. Leuk. Lymphoma, *37:* 53–63, 2000.
5. Jing, Y., Dai, J., Chalmers-Redman, R. M., Tatton, W. G., and Waxman, S. Arsenic trioxide selectively induces acute promyelocytic leukemia cell apoptosis via a hydrogen peroxide-dependent pathway. Blood, *94:* 2102–2111, 1999.
6. Bode, A., and Dong, Z. Apoptosis induction by arsenic: mechanisms of action and possible clinical applications for treating therapy-resistant cancers. Drug Resist. Updat., *3:* 21–29, 2000.
7. Bode, A. M., and Dong, Z. The paradox of arsenic: molecular mechanisms of cell transformation and chemotherapeutic effects. Crit. Rev. Oncol. Hematol., *42:* 5–24, 2002.
8. Dai, J., Weinberg, R. S., Waxman, S., and Jing, Y. Malignant cells can be sensitized to undergo growth inhibition and apoptosis by arsenic trioxide through modulation of the glutathione redox system. Blood, *93:* 268–277, 1999.
9. Cai, X., Shen, Y-L., Zhu, Q., Jia, P-M., Yu, Y., Zhou, L., Huang, Y., Zhang, J-W., Xiong, S-M., Chen, S-J., Wang, Z-Y., Chen, Z., and Chen, G-Q. Arsenic trioxide-induced apoptosis and differentiation are associated respectively with mitochondrial transmembrane potential collapse and retinoic acid signaling pathway in acute promyelocytic leukemia. Leukemia (Baltimore), *14:* 262–270, 2000.
10. Yi, J., Gao, F., Shi, G., Li, H., Wang, Z., Shi, X., and Tang, X. The inherent cellular level of reactive oxygen species: one of the mechanisms determining apoptotic susceptibility of leukemic cells to arsenic trioxide. Apoptosis, *7:* 209–215, 2002.
11. Gao, F., Yi, J., Shi, G. Y., Li, H., Shi, X. G., and Tang, X. M. The sensitivity of digestive tract tumor cells to As_2O_3 is associated with the inherent cellular level of reactive oxygen species. World J. Gastroenterol., *8:* 36–39, 2002.
12. Akao, M., Teshima, Y., and Marban, E. Antiapoptotic effect of nicorandil mediated by mitochondrial ATP-sensitive potassium channels in cultured cardiac myocytes. J. Am. Coll. Cardiol., *40:* 803–810, 2002.
13. Xie, P., Browning, D. D., Hay, N., Mackman, N., and Ye, R. D. Activation of NF-κB by bradykinin through a $G\alpha_q$- and $G\beta\gamma$-dependent pathway that involves phosphoinositide 3-kinase and Akt. J. Biol. Chem., *275:* 24907–24914, 2000.
14. Ye, R. D., Pan, Z., Kravchenko, V. V., Browning, D. D., and Prossnitz, E. R. Gene transcription through activation of G-protein-coupled chemoattractant receptors. Gene Expr., *5:* 205–215, 1996.
15. Kravchenko, V. V., Pan, Z., Han, J., Herbert, J. M., Ulevitch, R. J., and Ye, R. D. Platelet-activating factor induces NF-κB activation through a G protein-coupled pathway. J. Biol. Chem., *270:* 14928–14934, 1995.
16. Pecere, T., Gazzola, M. V., Mucignat, C., Parolin, C., Vecchia, F. D., Cavaggioni, A., Basso, G., Diaspro, A., Salvato, B., Carli, M., and Palu, G. Aloe-emodin is a new type of anticancer agent with selective activity against neuroectodermal tumors. Cancer Res., *60:* 2800–2804, 2000.
17. De Flora, S., Izzotti, A., D'Agostini, F., and Balansky, R. M. Mechanisms of *N*-acetylcysteine in the prevention of DNA damage and cancer, with special reference to smoking-related end-points. Carcinogenesis (Lond.), *22:* 999–1013, 2001.
18. Mayer, M., and Noble, M. *N*-Acetyl-L-cysteine is a pluripotent protector against cell death and enhancer of trophic factor-mediated cell survival *in vitro*. Proc. Natl. Acad. Sci. USA, *91:* 7496–7500, 1994.
19. Chan, T. C., Chang, C. J., Koonchanok, N. M., and Geahlen, R. L. Selective inhibition of the growth of ras-transformed human bronchial epithelial cells by emodin, a

protein-tyrosine kinase inhibitor. Biochem. Biophys. Res. Commun., *193:* 1152–1158, 1993.
20. Kamei, H., Koide, T., Kojima, T., Hashimoto, Y., and Hasegawa, M. Inhibition of cell growth in culture by quinones. Cancer Biother. Radiopharm., *13:* 185–188, 1998.
21. Lee, H. Z. Effects and mechanisms of emodin on cell death in human lung squamous cell carcinoma. Br. J. Pharmacol., *134:* 11–20, 2001.
22. Huang, H. C., Chang, J. H., Tung, S. F., Wu, R. T., Foegh, M. L., and Chu, S. H. Immunosuppressive effect of emodin, a free radical generator. Eur. Pharmacol., *211:* 359–364, 1992.
23. Kuo, P., Lin, T., and Lin, C. The antiproliferative activity of aloe-emodin is through p53-dependent and p21-dependent apoptotic pathway in human hepatoma cell lines. Life Sci., *71:* 1879–1892, 2002.
24. Zhang, L., Lau, Y. K., Xia, W., Hortobagyi, G. N., and Hung, M. C. Tyrosine kinase inhibitor emodin suppresses growth of HER-2/neu-overexpressing breast cancer cells in athymic mice and sensitizes these cells to the inhibitory effect of paclitaxel. Clin. Cancer Res., *5:* 343–353, 1999.
25. Shi, M. M., Kugelman, A., Iwamoto, T., Tian, L., and Forman, H. J. Quinone-induced oxidative stress elevates glutathione and induces γ-glutamylcysteine synthetase activity in rat lung epithelial L2 cells. J. Biol. Chem., *269:* 26512–26517, 1994.
26. Liu, R. M., Shi, M. M., Giulivi, C., and Forman, H. J. Quinones increase γ-glutamyl transpeptidase expression by multiple mechanisms in rat lung epithelial cells. Am. J. Physiol., *274:* L330–L336, 1998.
27. Kovacic, P., and Osuna, J. A., Jr. Mechanisms of anti-cancer agents: emphasis on oxidative stress and electron transfer. Curr. Pharm. Des., *6:* 277–309, 2000.
28. Rahimipour, S., Bilkis, I., Peron, V., Gescheidt, G., Barbosa, F., Mazur, Y., Koch, Y., Weiner, L., and Fridkin, M. Generation of free radicals by emodic acid and its [D-Lys6]GnRH-conjugate. Photochem. Photobiol., *74:* 226–236, 2001.
29. Kroemer, G., and de The, H. Arsenic trioxide, a novel mitochondriotoxic anticancer agent? J. Natl. Cancer Inst. (Bethesda), *91:* 743–745, 1999.
30. Woo, S. H., Park, I. C., Park, M. J., Lee, H. C., Lee, S. J., Chun, Y. J., Lee, S. H., Hong, S. I., and Rhee, C. H. Arsenic trioxide induces apoptosis through a reactive oxygen species-dependent pathway and loss of mitochondrial membrane potential in HeLa cells. Int. J. Oncol., *21:* 57–63, 2002.
31. Sauer, H., Wartenberg, M., and Hescheler, J. Reactive oxygen species as intracellular messengers during cell growth and differentiation. Cell Physiol. Biochem., *11:* 173–186, 2001.
32. Finkel, T. Reactive oxygen species and signal transduction. IUBMB Life, *52:* 3–6, 2001.
33. Janssen-Heininger, Y. M., Poynter, M. E., and Baeuerle, P. A. Recent advances towards understanding redox mechanisms in the activation of nuclear factor κB. Free Radic. Biol. Med., *28:* 1317–1327, 2000.
34. Herr, I., and Debatin, K. M. Cellular stress response and apoptosis in cancer therapy. Blood, *98:* 2603–2614, 2001.
35. Hsu, T. C., Young, M. R., Cmarik, J., and Colburn, N. H. Activator protein 1 (AP-1)- and nuclear factor κB (NF-κB)-dependent transcriptional events in carcinogenesis. Free Radic. Biol. Med., *28:* 1338–1348, 2000.
36. Karin, M., and Shaulian, E. AP-1: linking hydrogen peroxide and oxidative stress to the control of cell proliferation and death. IUBMB Life, *52:* 17–24, 2001.
37. Shaulian, E., and Karin, M. AP-1 in cell proliferation and survival. Oncogene, *20:* 2390–2400, 2001.
38. Shaulian, E., and Karin, M. AP-1 as a regulator of cell life and death. Nat. Cell Biol., *4:* E131–E136, 2002.
39. Bian, X., McAllister-Lucas, L. M., Shao, F., Schumacher, K. R., Feng, Z., Porter, A. G., Castle, V. P., and Opipari, A. W., Jr. NF-κB activation mediates doxorubicin-induced cell death in N-type neuroblastoma cells. J. Biol. Chem., *276:* 48921–48929, 2001.
40. Bian, X., Opipari, A. W., Jr., Ratanaproeksa, A. B., Boitano, A. E., Lucas, P. C., and Castle, V. P. Constitutively active NF-κB is required for the survival of S-type neuroblastoma. J. Biol. Chem., *277:* 42144–42150, 2002.
41. Levkau, B., Scatena, M., Giachelli, C. M., Ross, R., and Raines, E. W. Apoptosis overrides survival signals through a caspase-mediated dominant-negative NF-κB loop. Nat. Cell Biol., *1:* 227–233, 1999.
42. Davis, R. J. Signal transduction by the JNK group of MAP kinases. Cell, *103:* 239–252, 2000.
43. Deng, X., Xiao, L., Lang, W., Gao, F., Ruvolo, P., and May, W. S., Jr. Novel role for JNK as a stress-activated Bcl2 kinase. J. Biol. Chem., *276:* 23681–23688, 2001.
44. Pearce, A. K., and Humphrey, T. C. Integrating stress-response and cell-cycle checkpoint pathways. Trends Cell Biol., *11:* 426–433, 2001.
45. Burdon, R. H. Control of cell proliferation by reactive oxygen species. Biochem. Soc. Trans., *24:* 1028–1032, 1996.
46. Greenberger, J. S., Kagan, V. E., Pearce, L., Boriseniao, G., Tyurina, Y., and Epperly, M. W. Modulation of redox signal transduction pathways in the treatment of cancer. Antioxid. Redox. Signal., *3:* 347–359, 2001.